



Temperature induced in the testicular and related tissues due to electromagnetic fields exposure at 900 MHz and 1800 MHz



Teerapot Wessapan^a, Phadungsak Rattanadecho^{b,*}

^a School of Aviation, Eastern Asia University, Pathumthani 12110, Thailand

^b Center of Excellence in Electromagnetic Energy Utilization in Engineering (CEEE), Department of Mechanical Engineering, Faculty of Engineering, Thammasat University (Rangsit Campus), Pathumthani 12120, Thailand

ARTICLE INFO

Article history:

Received 9 April 2016

Received in revised form 5 July 2016

Accepted 5 July 2016

Keywords:

Electromagnetic fields
Temperature increase
Specific absorption rate
Human testis
Heat transfer

ABSTRACT

Increased testicular temperature adversely affects the reproductive system in the male. Environmental conditions, namely high ambient temperature and electromagnetic fields (EMFs), influence the temperature increase in the human body. This study considers the computationally determined specific absorption rate (SAR) and the heat transfer in a piecewise-homogeneous human model of the male reproductive organs and upper thigh exposed to an electric dipole antenna. The study focuses on increases in testicular temperature due to EMF absorption. Much attention is paid to the effects of the operating frequency and exposure time on the SAR and temperature increases induced by exposure to a near-field EMF. The electric field, SAR and temperature distributions in various tissues during exposure to EMFs are obtained by numerical simulation of EM wave propagation and an unsteady bioheat transfer model. This study indicated that when the model is exposed to EMFs at the frequencies of 900 and 1800 MHz, the highest SAR values are obtained in the scrotum. In the testis, which is the most sensitive part of the male reproductive system, the SAR value of the 900 MHz frequency is significantly higher than that of 1800 MHz, while there are no significant differences in the temperature increases between the two operating frequencies. The obtained results may be of assistance in determining exposure limits for the power output of wireless transmitters, and their operating frequency for use with humans.

Significant of this work: The study focuses on increases in testicular temperature due to EMF absorption. Much attention is paid to the effects of the operating frequency and exposure time on the SAR and temperature increases induced by exposure to a near-field EMF. The electric field, SAR and temperature distributions in various tissues during exposure to EMFs are obtained by numerical simulation of EM wave propagation and an unsteady bioheat transfer model. The obtained results may be of assistance in determining exposure limits for the power output of wireless transmitters, and their operating frequency for use with humans.

© 2016 Elsevier Ltd. All rights reserved.

1. Introduction

In the male reproductive system, testicular function is temperature dependent. Normal testicular function requires a temperature of 2–4 °C below the body temperature [1–2]. It is reported that a very small temperature increase of 1 °C in the testicle may alter the production of sperm [3]. Scrotal temperature is also highly correlated with testicular temperature [4]. Elevated scrotal temperature is a well documented mechanism of abnormal spermatogenesis in common diseases associated with male infertility [5]. Scrotal hyperthermia produced by exposure to various heat

sources, such as laptop computers [6] and scrotal insulation [7], has been studied.

In recent years, the utilization of electromagnetic (EM) waves in various applications has been increasing rapidly in daily life, including mobile phones, tablet, laptops and microwave cooking. The high intensity EM fields of different power levels and frequencies penetrate deep into the human body and raise the temperature in the tissues, causing health risks. The concern is heightened when the power absorption in the male genital area and the sensation of warmth for the testis and skin in close proximity to the intense radiation source induces a temperature increase inside it. While the testicles are well known to be very sensitive to heat, portable devices are commonly used on the lap; therefore the genital area is subjected to EM fields and transferred heat [8–11]. However, the resulting thermo-physiological

* Corresponding author.

E-mail addresses: teerapot@eau.ac.th (T. Wessapan), ratphadu@engr.tu.ac.th (P. Rattanadecho).

Nomenclature

C	specific heat capacity (J/(kg K))
E	electric field intensity (V/m)
f	frequency of incident wave (Hz)
H	magnetic field (A/m)
h	convection coefficient (W/m ² K)
j	current density (A/m ²)
k	thermal conductivity (W/(m K))
n	normal vector
Q	heat source (W/m ³)
T	temperature (K)
t	time

Greek letters

μ	magnetic permeability (H/m)
-------	-----------------------------

ε	permittivity (F/m)
σ	electric conductivity (S/m)
ω	angular frequency (rad/s)
ρ	density (kg/m ³)
ω_b	blood perfusion rate (1/s)

Subscripts

b	blood
ext	external
met	metabolic
r	relative
0	free space, initial condition

response of the reproductive organs and related tissue to EM fields is still not well understood. In order to gain insight into the phenomena in the reproductive organs related to the temperature increase induced by EM fields, a detailed knowledge of the absorbed power distribution as well as the temperature distribution is necessary. Therefore, this study aims to investigate the interaction effects between EMF and tissues that occur during exposure to EM waves. Although safety standards in terms of the maximum SAR values are regulated [12], they are not stated in terms of the maximum temperature increase in the tissue caused by EM energy absorption, which is the actual influence of the dominant factors inducing adverse physiological effects. Numerical analysis of the heat transfer in male reproductive organs exposed to EM fields has provided useful information on the absorption of EM energy under a variety of exposure conditions.

The thermal modeling of human tissue is important as a tool to investigate the effect of external heat sources and to predict abnormalities in the tissue. The modeling of heat transport in human tissue was first introduced by Pennes [13] based on the heat diffusion equation. The equation is normally called Pennes' bioheat equation and is frequently used for the analysis of heat transfer in human tissues. The topic of temperature increases in human tissue caused by exposure to EM waves has been of interest for several years. There are some experimental studies in animals such as rat [14], cow [15] and pig [16]. However, the results may not represent the practical behavior of human tissues. Our research group has numerically investigated the temperature increase in human tissue subjected to EMFs in many studies [17–27]. Wessapan et al. [17,18] utilized a 2D finite element method (FEM) to obtain the specific absorption rate (SAR) and temperature increase in the human body exposed to leaked EM waves. Wessapan et al. [19,20] developed a 3D model of the human head in order to investigate the SAR and temperature distributions in the human head during exposure to mobile phone radiation. Keangin et al. [21–22] carried out a numerical simulation of liver cancer treated using a complete mathematical model that considered the coupled model of EM wave propagation and heat transfer. Moreover, an analysis of mechanical deformation in the biological tissue with a microwave ablation was investigated [23]. Wessapan et al. [24–27] investigated the SAR and temperature distributions in the eye during exposure to EM waves based on the porous media theory. Although many advanced transport models of biological tissue have been proposed, Pennes' bioheat model is still a good approximation and widely used for modeling the heating of biological tissue because of its easy implementation and minimum data requirement.

Calculating the spatially-induced electric field and SAR becomes more complex when the human body is non-uniform in shape and contains several parts. Most studies of the human body's exposure to EM waves have not considered a realistic domain with complicated organs of several types of tissue, especially in the reproductive system, and experimental validation is limited or non-existent. Therefore, in order to provide information on the levels of exposure and health effects from EM radiation, it is essential to simulate both the EM field and heat transfer within an anatomically based human body model to represent the actual processes of heat transfer within the human organ.

This study presents the simulation of the SAR and temperature increases in a male reproductive system model exposed to an electric dipole antenna. A two-dimensional human model was used to simulate the SAR and the temperature increases induced by EM energy. The model comprises seven types of tissue: the skin, fat, muscle, bone, testis, penis and scrotum. The EM wave propagation was investigated by using Maxwell's equations. An analysis of the heat transfer was investigated using a bioheat transfer model. In the piecewise-homogeneous human model, the effect of operating frequency on the SAR and temperature distributions in each tissue layer is systematically investigated. In this study, the frequencies of 900 and 1800 MHz are chosen for our simulations as the frequencies used globally in a wide range of applications including Global System for Mobile Communications (GSM) services. In this work, the model excluded the presence of clothing in order to ease the modeling procedures. The values obtained represent the accurate phenomena to determine the temperature increase in the male reproductive organs and indicate the limitations that must be considered as the temperature increases due to EM energy absorption from EM field exposure at different frequencies.

2. Formulation of the problem

Whether or not electromagnetic (EM) fields induced from a strong near-field source potentially pose any direct or indirect health hazards for humans is uncertain. Further, the human body's response to thermo-physiological phenomena is currently not well understood. Near-field sources such as mobile phones and portable wireless routers operate in the close vicinity of the body and can cause temporarily high local exposure. For adequate study of the transport phenomena in human tissue caused by EM near-field exposures, the contribution of different EM sources to the human exposure of different body tissues is required. Fig. 1 shows human

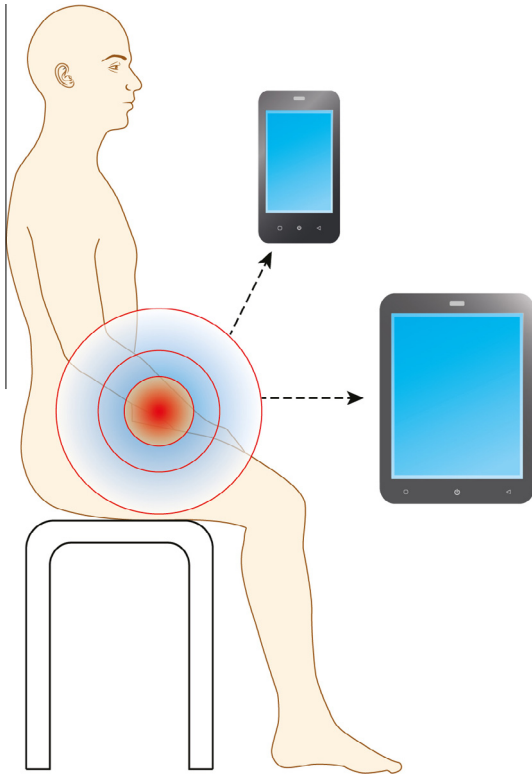


Fig. 1. Human exposure to near-field EM radiation.

exposure to near-field EM radiation. Due to ethical considerations, exposures of the human to EM fields for experimental purposes are limited. It is more convenient to develop a realistic human model through numerical simulation. A highlight of this work is the illustration of the heat transfer in a piecewise-homogeneous human model of the male reproductive organs and upper thigh exposed to EMFs at different frequencies. The analyses of the SAR and the heat transfer in the model will be illustrated in Section 3. The system of governing equations as well as the initial and boundary conditions are solved numerically using the finite element method (FEM) via COMSOLTM Multiphysics.

3. Methods and model

The first step in evaluating the effects of a certain exposure to EM fields in the human body is to determine the induced internal EM fields and their spatial distribution. Thereafter, EM energy absorption which results in a temperature increase in the human body and other interactions can be considered. This study considers the heat transfer and temperature increases of such exposure and their implications for the threshold for EM hazard.

3.1. Physical model

In order to investigate the effects of EM near-field exposure on the body and male reproductive system, a piecewise-homogeneous human model of the male reproductive organs and upper thigh is exposed to an electric dipole antenna. In this study, a 2D model is considered in order to minimize the amount of computational time while maintaining resolution.

Fig. 2 shows the physical domain of this study, in which interactions between the human body and the dipole antenna take place. In the model, the thighs are 15 cm in diameter. The testicles have the dimensions of 3 cm in length and 2 cm in width. The skin and fat layer have thicknesses of 2 mm and 5 mm respectively. The

femur bone and penis have diameters of 4 cm and 3 cm respectively. This model comprises seven types of tissue: the skin, fat, muscle, bone, testis, penis and scrotum. These tissues have different dielectric and thermal properties. The dielectric and thermal properties are obtained according to the comprehensive literature review of Hasgall [29] (www.itis.ethz.ch/database), the dielectric properties of which are largely identical to those proposed by Gabriel et al. [30]. The dielectric and thermal properties of the tissues are given in Tables 1 and 2, respectively. Each tissue is assumed to be homogeneous and electrically as well as thermally isotropic. There is no effect on the chemical reaction and phase change within the tissue. The antenna's feed point, located at the middle of the thighs with a certain position, is considered as a near-field radiation source for the human body. The antenna is excited at the center feed point, and the transmitted power is determined as the complex product of the current and voltage at the feed point. The dipole used operates at 900 and 1800 MHz frequencies and transmits the radiated power of 2.0 W, the approximate maximum output of general mobile phone and wireless transmitters.

3.2. Equations for EM wave propagation analysis

The mathematical models are developed to predict the electric fields and the SAR with respect to the temperature gradient in the model. To simplify the problem, the following assumptions are made:

1. The EM wave propagation is modeled in two dimensions.
2. The EM wave interaction with the tissue proceeds in the open region.
3. The free space is truncated by a scattering boundary condition.
4. The model assumes that the dielectric properties of each tissue are constant.
5. The radiated waves from the dipole are characterized by transverse electric (TE) fields.

The EM wave propagation is calculated using Maxwell's equations [17], which mathematically describe the interdependence of the EM waves. The general form of Maxwell's equations is simplified to demonstrate the EM field that penetrates into the tissue as follows:

$$\nabla \times \left(\frac{1}{\mu_r} \nabla \times E \right) - k_0^2 \left(\epsilon_r - \frac{j\sigma}{\omega\epsilon_0} \right) E = 0 \quad (1)$$

$$\epsilon_r = n^2 \quad (2)$$

where E is the electric field intensity (V/m), μ_r is the relative magnetic permeability, n is the refractive index, ϵ_r is the relative dielectric constant, $\epsilon_0 = 8.8542 \times 10^{-12}$ F/m is the permittivity of free space, is the electric conductivity (S/m), $j = \sqrt{-1}$ and k_0 is the free space wave number (m^{-1}).

3.2.1. Boundary condition for wave propagation analysis

The boundary conditions along the interfaces between different mediums, namely, between air and tissue, are considered as a continuity boundary condition:

$$n \times (H_1 - H_2) = 0 \quad (3)$$

The outer sides of the calculated domain, i.e., free space, are considered as a scattering boundary condition to eliminate reflections:

$$n \times (\nabla \times E) - jkE = 0 \quad (4)$$

where k is the wave number (m^{-1}), n is the normal vector, $j = \sqrt{-1}$, and H is the magnetic field (A/m).

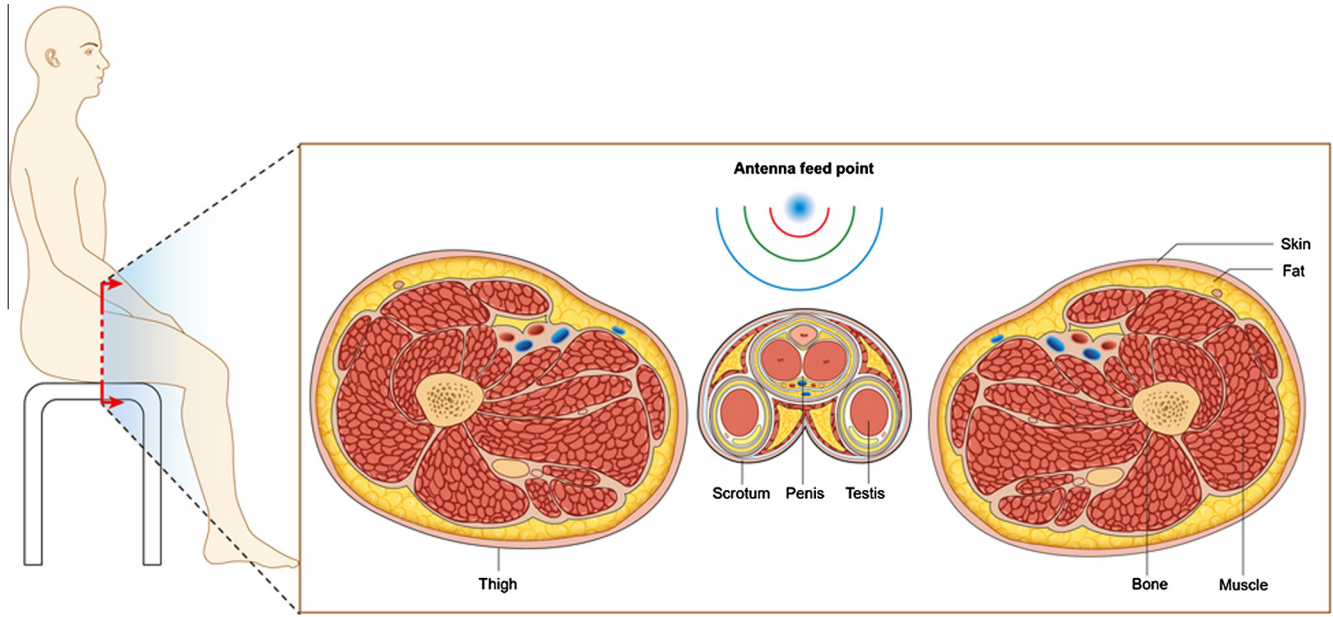


Fig. 2. The physical domain of the problem.

Table 1
Dielectric properties of tissues [29,30].

	900 MHz		1800 MHz	
	ϵ_r	σ (S/m)	ϵ_r	σ (S/m)
Skin	41.4	0.867	38.9	1.18
Fat	11.3	0.109	11.0	0.19
Muscle	55.0	0.943	53.5	1.34
Bone	12.5	0.143	11.8	0.275
Testis	60.6	1.21	58.6	1.69
Penis	44.8	0.696	43.3	1.07
Scrotum	41.4	0.867	38.9	1.18

3.3. Interaction of EM fields and human tissues

To quantify the exposure conditions and the resulting responses for the various biological tissues, the specific absorption rate (SAR) is used. When the EM waves propagate through the tissue, the energy of the EM waves is absorbed by the tissue. The SAR is critical to the antenna design, because if the SAR is too high the antenna must be changed. The SAR is defined as the power dissipation rate normalized by the material density. The SAR is given by

$$SAR = \frac{\sigma}{\rho} |E|^2 \tag{5}$$

where E is the electric field intensity (V/m), σ is the electric conductivity (S/m), and ρ is the tissue density (kg/m³).

Table 2
Thermal properties of tissues [29].

Tissue	ρ (kg/m ³)	k (W/m°C)	C (J/kg°C)	Q_{met} (W/m ³)	ω_b (1/s)
Skin	1109	0.37	3391	1829	1.59e-3
Fat	911	0.21	2348	464.6	6.03e-4
Muscle	1090	0.49	3421	991.9	5.65e-4
Bone (cortical/compact bone)	1908	0.32	1313	162.3	8.73e-5
Testis	1082	0.52	3778	343	3.08e-3
Penis	1102	0.46	3306	209.38	1.81e-4
Scrotum	1109	0.37	3391	1829	1.59e-3
Blood	1050	0.52	3617	-	-

3.4. Equations for heat transfer analysis

To solve the thermal problem, the coupled effects of the EM wave propagation and the unsteady bioheat transfer are investigated. The temperature distribution corresponds with the SAR. This is because the SAR in the tissue is distributed owing to energy absorption. Thereafter, the electromagnetic absorbed energy is converted to thermal energy, which increases the tissue temperature. To reduce the complexity of the problem, the following assumptions are made:

1. The tissue is a bio-material with constant thermal properties.
2. There is no phase change of substance in the tissue.
3. There is no energy exchange throughout the outer surface of the human model.
4. There is no chemical reaction in the tissue.
5. The heat transfer is modeled in two dimensions.
6. The thermal properties of the tissues are constant.

The temperature increase within the human body is obtained by solving Pennes' bio-heat equation [13]. The transient bioheat equation describes effectively how heat transfer occurs within the tissue, and the equation can be written as

$$\rho C \frac{\partial T}{\partial t} = \nabla \cdot (k \nabla T) + \rho_b C_b \omega_b (T_b - T) + Q_{met} + Q_{ext} \tag{6}$$

where ρ is the tissue density (kg/m³), C is the heat capacity of tissue (J/kg K), k is the thermal conductivity of tissue (W/m K), T is the tis-

sue temperature ($^{\circ}\text{C}$), T_b is the temperature of blood ($^{\circ}\text{C}$), ρ_b is the density of blood (kg/m^3), C_b is the heat capacity of blood ($\text{J}/\text{kg K}$), ω_b is the blood perfusion rate ($1/\text{s}$), Q_{met} is the metabolism heat source (W/m^3) and Q_{ext} is the external heat source (electromagnetic heat-source density) (W/m^3).

In the analysis, heat conduction between the tissue and blood flow is approximated by the blood perfusion term, $\rho_b C_b \omega_b (T_b - T)$.

The external heat source term is equal to the resistive heat generated by the electromagnetic field (electromagnetic power absorbed), which is defined as

$$Q_{ext} = \frac{1}{2} \sigma_{tissue} |\bar{E}|^2 = \frac{\rho}{2} \cdot SAR \quad (7)$$

3.4.1. Boundary condition for heat transfer analysis

Heat transfer is considered only in the human model, which does not include parts of the surrounding space. As shown in Fig. 3, the outer surface of the human model, corresponding to assumption (3), is considered to be a thermally insulated boundary condition:

$$n \cdot (k \nabla T) = 0 \quad (8)$$

It is assumed that no contact resistance occurs between the layers of the human tissue. Therefore, the internal boundaries are assumed to be continuous:

$$n \cdot (k_u \nabla T_u - k_d \nabla T_d) = 0 \quad (9)$$

$$T_u = T_d \quad (10)$$

3.5. Calculation procedure

In this study, the finite element formulations of the coupled electromagnetic–bioheat transfer model in the human body are carried out over the entire domain. In order to obtain a good approximation, a fine mesh is specified in the sensitive areas. This study provides a variable mesh method for solving the problem, as shown in Fig. 3. The system of governing equations as well as the initial and boundary conditions are then solved. All computational processes are implemented using COMSOLTM Multiphysics, to demonstrate the phenomenon that occurs in the organs exposed to the EM fields.

The 2D model is discretized using triangular elements and the Lagrange quadratic elements are then used to approximate the

temperature and SAR variations across each element. A grid independence test is carried out to identify the appropriate number of elements required. This grid independence test leads to a mesh with approximately 40,000 elements. It is reasonable to assume that, at this element number, the accuracy of the simulation results is independent of the number of elements.

4. Results and discussion

The numerical analysis of coupled electromagnetic propagation and heat transfer is done by solving the Maxwell and bioheat equations. The dielectric and thermal properties are taken directly from Tables 1 and 2 respectively. The exposed radiated power used in this study refers to the International Commission of Non-Ionizing Radiation Protection (ICNIRP) standard for safety levels at the maximum SAR value of 2 W/kg (general public exposure) and 10 W/kg (occupational exposure) [12]. Since, in mobile communication, GSM-900 and GSM-1800 are used in most parts of the world, therefore in this analysis, the effects of these operating frequencies on the distributions of the SAR and temperature increase in the organs are systematically investigated.

4.1. Verification of the model

Before we can solve the problem, an initial numerical validation is required to support the results stated within this paper. In order to verify the accuracy of the present numerical models, the simple case of the simulated results is validated against the numerical results obtained with the same geometric model obtained by Riu and Foster [28]. The SAR is determined in a homogeneous tissue model from near-field exposure to a dipole antenna. In the validation case, the dipole used operates at 900 MHz frequency and transmits the radiated power of 0.6 W. The result of the validation test case is illustrated in Fig. 4 and clearly shows good agreement of the SAR value of the tissue between the present solution and that of Riu. The SAR decreases exponentially in the direction of wave propagation. This favorable comparison lends confidence in the accuracy of the present numerical model and ensures that the numerical model can accurately represent the phenomena occurring at the interaction of the EM fields with the tissue.

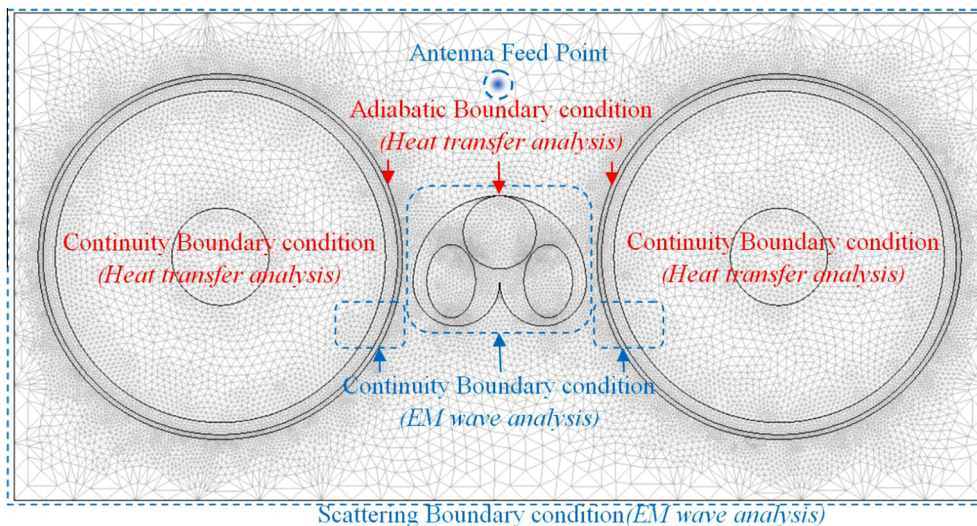


Fig. 3. Boundary condition for analysis of EM wave propagation and heat transfer.

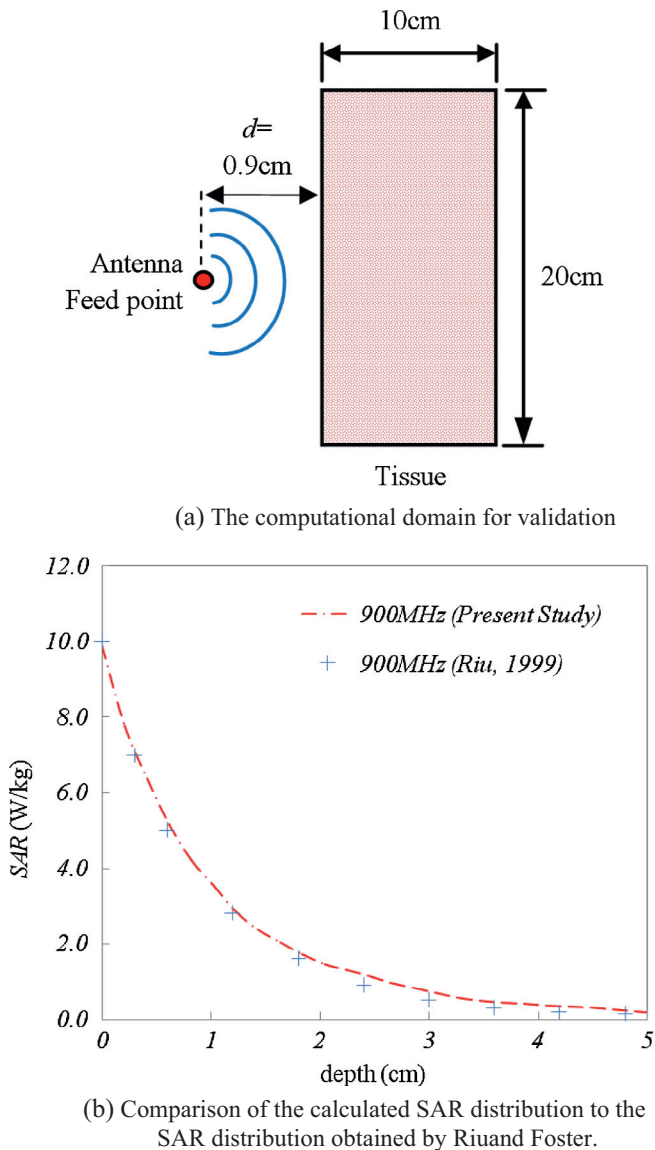


Fig. 4. Validation of the mathematical model: (a) The computational domain for validation; (b) Comparison of the calculated SAR distribution to the SAR distribution obtained by Riu and Foster [28].

4.2. Electric field distribution

In the model, the effect of the operating frequency on the electric field distribution is systematically investigated. The model is exposed to the dipole source at the frequencies of 900 and 1800 MHz to illustrate the penetrated electric field distribution inside the body. Fig. 5 shows the simulation of an electric field pattern inside the model exposed to the EM fields in TE mode operating at the frequencies of 900 and 1800 MHz and propagating over the vertical cross-section of the human model. Due to the different dielectric characteristics of the various tissue layers at different operating frequencies, a different fraction of the supplied EM energy will become absorbed in each layer in the model. Consequently, the reflection and transmission components at each layer contribute to the resonance of the standing wave in the tissue. It can be seen that the highest values of electric fields at both frequencies occur in the outer area of the body, especially in the penis and skin. By comparison, the maximum electric field intensity in the outer parts of the body at the frequency of 900 MHz displays

a higher value than that of 1800 MHz. The maximum electric field intensities are 124.735 and 115.395 V/m at the frequencies of 900 and 1800 MHz respectively. For both frequencies, the electric fields deep inside the muscle and bone are extinguished as the electric fields attenuate due to the absorbed EM energy and are then converted to heat. As shown in the figure, the penetration depth of the EM field inside the dispersive lossy tissue decreases as the frequency increases. The electric field at lower frequencies is attenuated at lower rates, which allow them to penetrate deeper into the tissue.

4.3. SAR distribution

Fig. 6 shows the SAR distribution evaluated on the vertical cross-section of the human model exposed to the EM frequencies of 900 and 1800 MHz. Even though the electric field intensity within the 900 MHz model is higher than that of 1800 MHz (Fig. 5), the maximum SAR value of 1800 MHz is higher than that of 900 MHz (Fig. 6). This is because the SAR is a function of the electrical conductivity, which corresponds to Eq. (5), and the increase in operating frequency causes the electrical conductivity to increase (Table 1), thereby increasing the SAR. The results of the SAR values in the model (Fig. 6) are increased in correspondence with the electric field intensities (Fig. 5). Besides the electric field intensity, the magnitude of the dielectric and thermal properties in each tissue will directly affect the SAR values in each organ.

For both frequencies, the highest SAR values are obtained in the penis and skin surface. For the radiated power of 2 W, the calculated maximum SAR values of the frequencies of 900 and 1800 MHz are 6.745 and 7.856 W/kg respectively. The main reason is the position of the penis and skin located close to the dipole source, at which the electric field intensity is strongest. Moreover, the penis and skin have a high dielectric constant value (ϵ), which means that the propagating EM energy can be absorbed, producing localized heating.

It is found that the SAR distribution pattern in the model, which corresponds to Eq. (5), depends on the effect of the electrical conductivity (σ , shown in Table 1) and tissue density (ρ , shown in Table 2). Moreover, the SAR distribution at the frequency of 900 MHz shows a greater value of EM power absorption in the deep part of the body, namely, in the testis. This is because the electric field at lower frequencies is attenuated at lower rates, which allow them to penetrate deeper into the tissue. Compared to the ICNIRP standard for the safety level at the maximum SAR value of 2 W/kg (general public exposure) [12], the resulting SAR values at both the 900 MHz and 1800 MHz frequencies are higher than the ICNIRP exposure limits for general public exposure.

4.4. Temperature distribution

Since this study has focused on the electromagnetic heating effect in the piecewise-homogeneous human model of the male reproductive system, the effects of an ambient temperature variation have been neglected in order to gain insight into the interaction between the EM fields and the tissue, as well as the correlation between the SAR and the heat transfer mechanism. Therefore, at the outer surface of the model, the adiabatic boundary condition provided by clothing is applied. The effect of thermoregulation mechanisms has also been neglected due to the small temperature increase that occurs during the exposure process.

In order to study the heat transfer in the tissue, the coupled effects of EM wave propagation and unsteady heat transfer as well as the initial and boundary conditions are then investigated. Due to these coupled effects, the electric field distribution in Fig. 5 and the SAR distribution in Fig. 6 are then transformed into an incremental

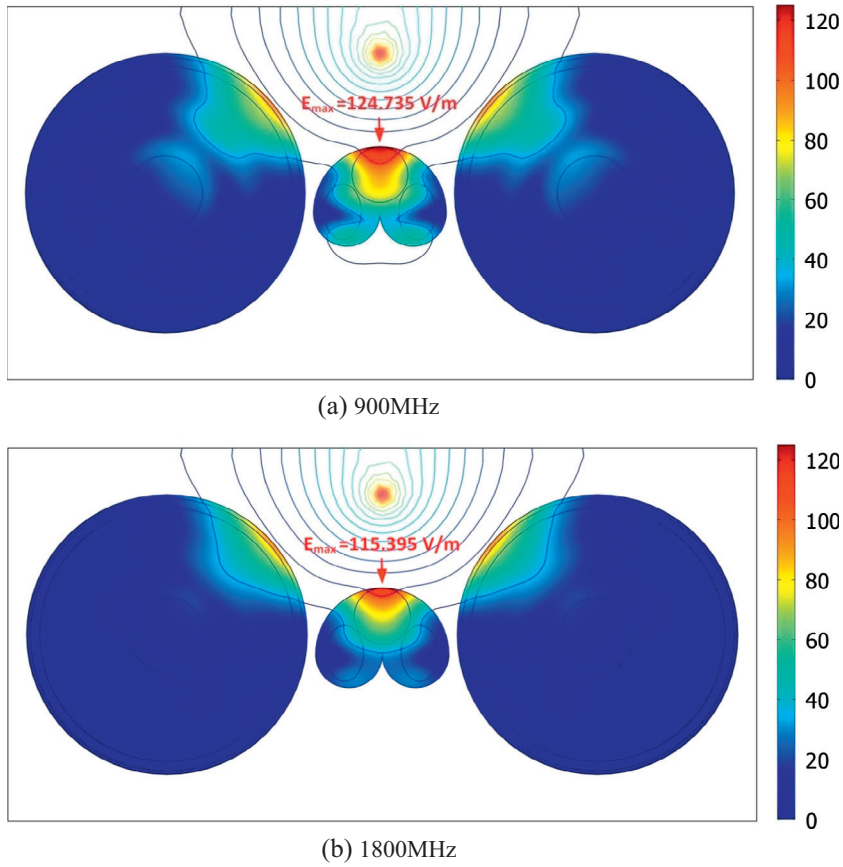


Fig. 5. Electric field distribution (V/m) in the human model exposed to the radiated powers of (a) 900 MHz (b) 1800 MHz.

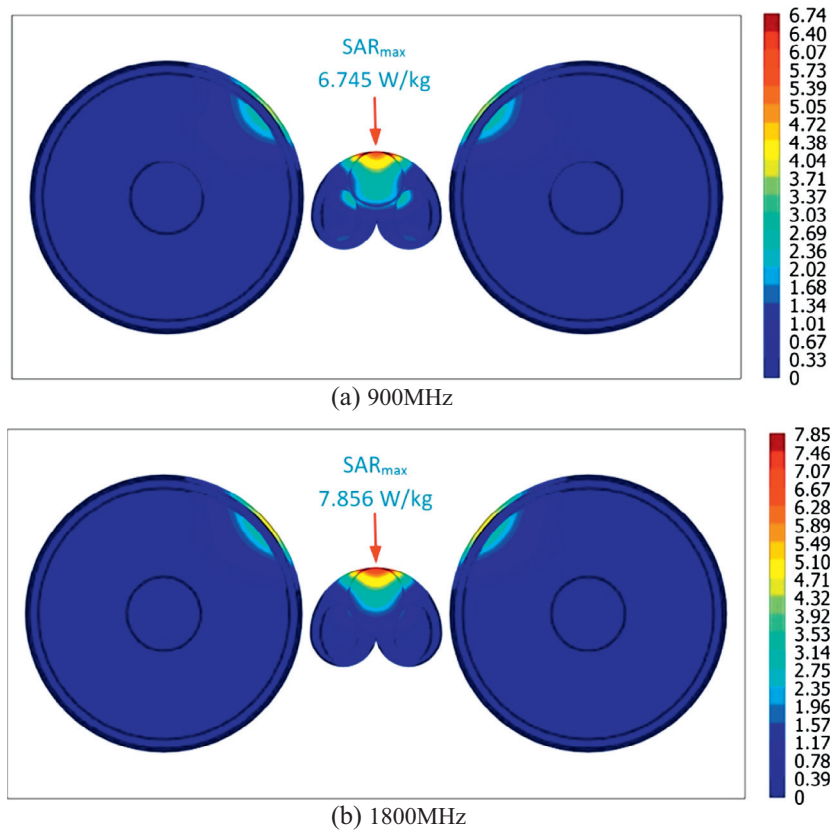


Fig. 6. SAR distribution (W/kg) in the human model exposed to the radiated power of 2 W at the frequencies of (a) 900 MHz (b) 1800 MHz.

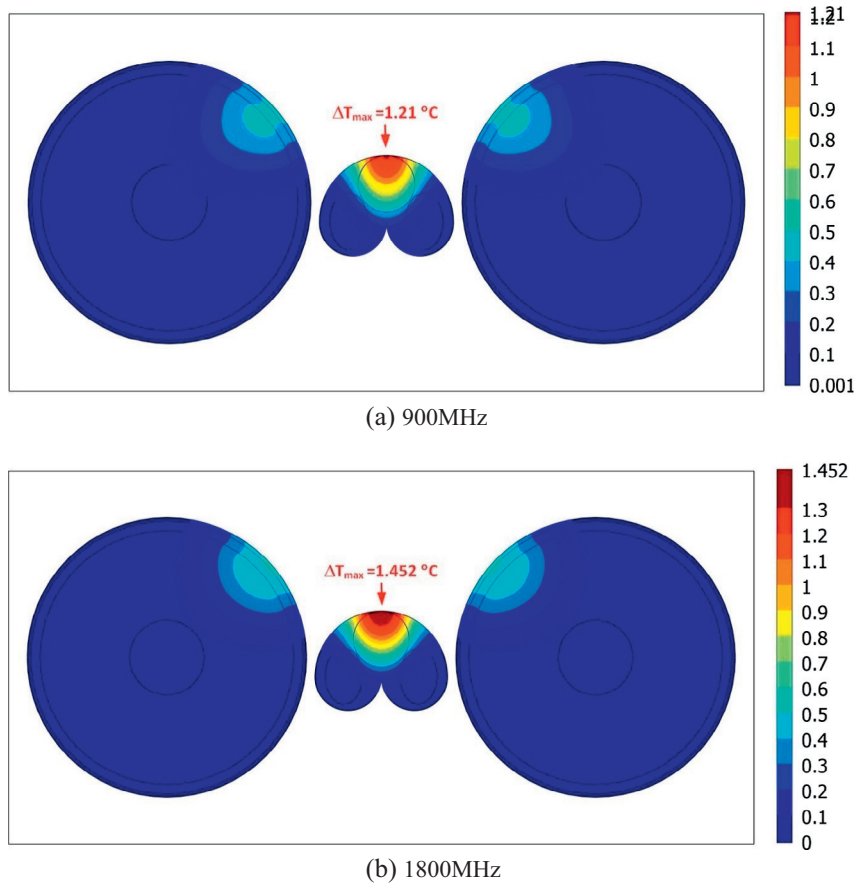


Fig. 7. The temperature increase (°C) at 60 min in the human model exposed to the radiated power of 2 W at the frequencies of (a) 900 MHz (b) 1800 MHz.

amount of heat by EMF absorption of the tissue. Fig. 7 shows the temperature increase in the vertical cross-section human model at 60 min of exposure to the EM radiated power of 2 W at the frequencies of 900 MHz (Fig. 7a) and 1800 MHz (Fig. 7b). For the model exposed to the EMF for 60 min, the tissue temperature (Fig. 7) is increased corresponding to the SAR (Fig. 6). This is because the electric fields in the tissue attenuate owing to the energy absorbed and thereafter the absorbed energy is converted to thermal energy, which increases the body temperature. It is found that when the model is subjected to the EM fields at

different frequencies, the distribution patterns of the temperature at a particular time are quite different. This is because the difference in the temperature distribution pattern between the two chosen frequencies is caused by the dielectric properties of the tissue as well as the electric field distribution pattern, which become the dominant mechanisms for the heat transfer.

Fig. 8 shows the comparison of the maximum SAR in each tissue type at the frequencies of 900 MHz and 1800 MHz. For both frequencies, the three highest SARs are shown for the scrotum, penis and skin. Furthermore, the localized SARs of the 1800 MHz

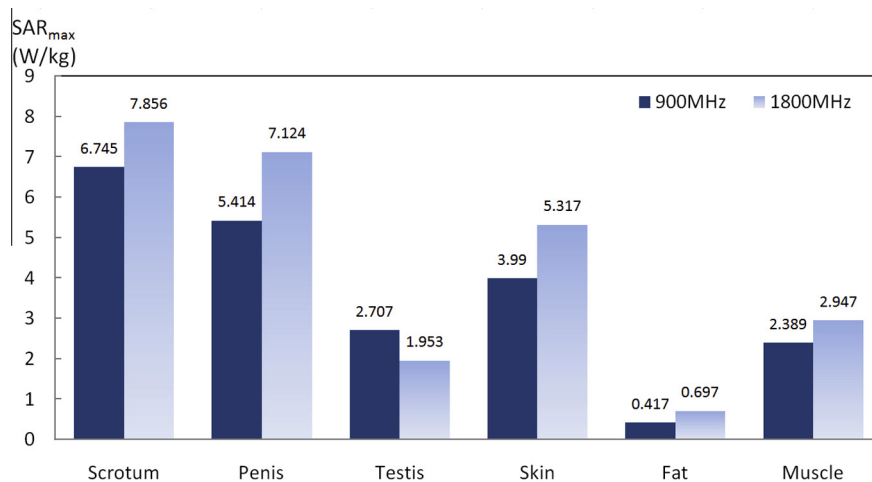


Fig. 8. Comparison of the maximum SAR (W/kg) in each tissue type at the frequencies of 900 MHz and 1800 MHz.

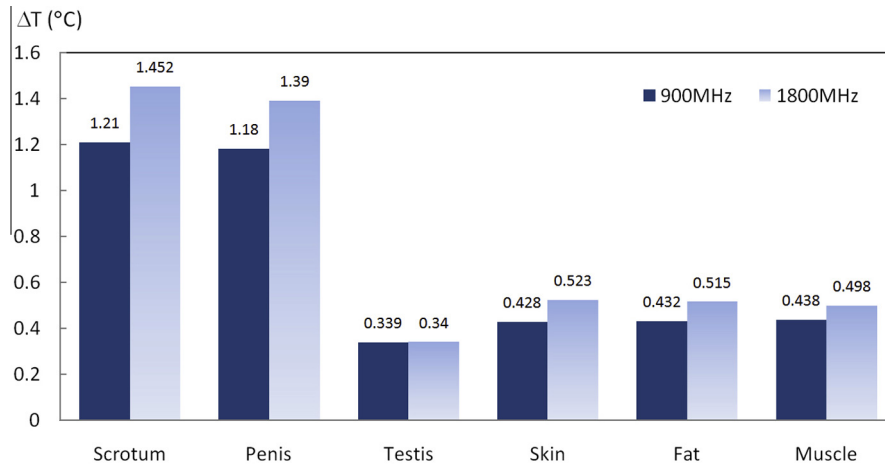


Fig. 9. Comparison of the temperature increase (°C) in each tissue type at the frequencies of 900 MHz and 1800 MHz.

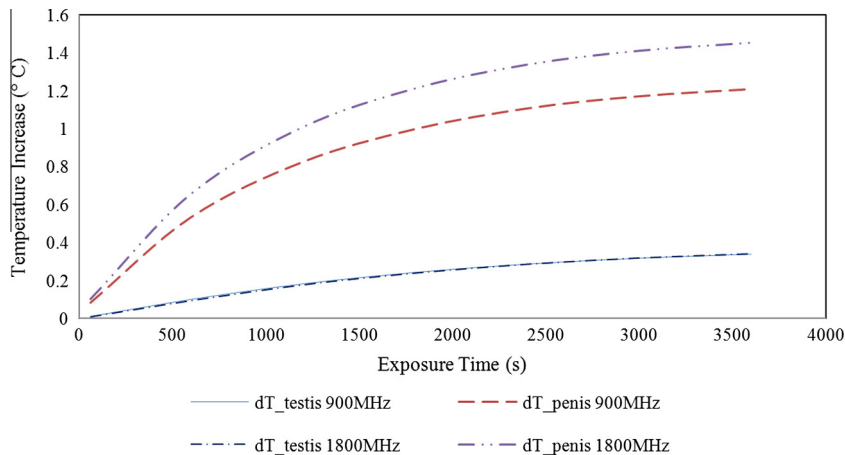


Fig. 10. Comparison of the temperature increase (°C) in testis and penis at various exposure times.

frequency are higher than the 900 MHz frequency in all organs except the testis. This is because the penetration depth of the 900 MHz frequency is larger than the 1800 MHz frequency and the testis position lies in the scrotum at the location of the deep inguinal ring.

The SAR values in Fig. 8 are then converted into heat through absorption by the tissues. Fig. 9 shows the comparison of the temperature increase in each tissue type at the frequencies of 900 MHz and 1800 MHz. The highest temperature increase in both frequencies occurs in the scrotum. The highest temperature increase in both frequencies also appears in the penis, corresponding to the SAR values. In the testis, it is observed that the 900 MHz frequency has higher SAR values than those at 1800 MHz (Fig. 8), while there is no significant difference in the temperature increases between 900 and 1800 MHz in the testis (Fig. 9). This is because at 1800 MHz, there is the contribution of heat conduction from the surrounding tissues with a higher temperature, namely the scrotum and penis, which displays a strong influence on the testis temperature. Moreover, the testis tissue also has a higher thermal conductivity (k), as shown in Table 2, which leads to increasing heat conduction from the surrounding tissue into the testis. It is found that the temperature distributions in the testis are not directly proportional to the local SAR values due to the effect of the interaction among parameters such as the thermal conductivity, dielectric properties, blood perfusion rate, etc.

Fig. 10 shows the comparison of the temperature increase in the testis and penis, which are the most sensitive parts of a man to EMFs, at various exposure times. From Fig. 10, it is found that the exposure time significantly influences the temperature increase in the testis and penis. A longer exposure time resulted in a higher heat accumulation in the tissue, thereby increasing its temperature. The temperature increase of the penis at a frequency of 1800 MHz is found to be higher than that at 900 MHz over the exposure time. In this case, the temperature increase varies according to the distribution of the electric fields and SAR. Due to the deeper penetration of the electric field of the 900 MHz frequency (Fig. 6a), it has a higher SAR value in the testis than that of 1800 MHz frequency, as shown in Fig. 8. However, there is no significant difference in the temperature increases between 900 and 1800 MHz in the testis over the exposure period (Fig. 10). This is because the thermal conduction from the surrounding tissue increases the temperature of the testis tissue at 1800 MHz.

Fig. 11 shows the comparison between the distribution of the SAR and the temperature increase in the testis during exposure to 900 and 1800 MHz EMF at the radiated power of 10 W at various exposure times. The maximum SAR values at 900 and 1800 MHz are 12.952 and 9.634 W/kg respectively. From the figure, the SAR distribution patterns show a wavy behavior, which varies corresponding to the wave patterns produced in the tissue. At the operating frequency of 900 MHz, the maximum temperature increases are

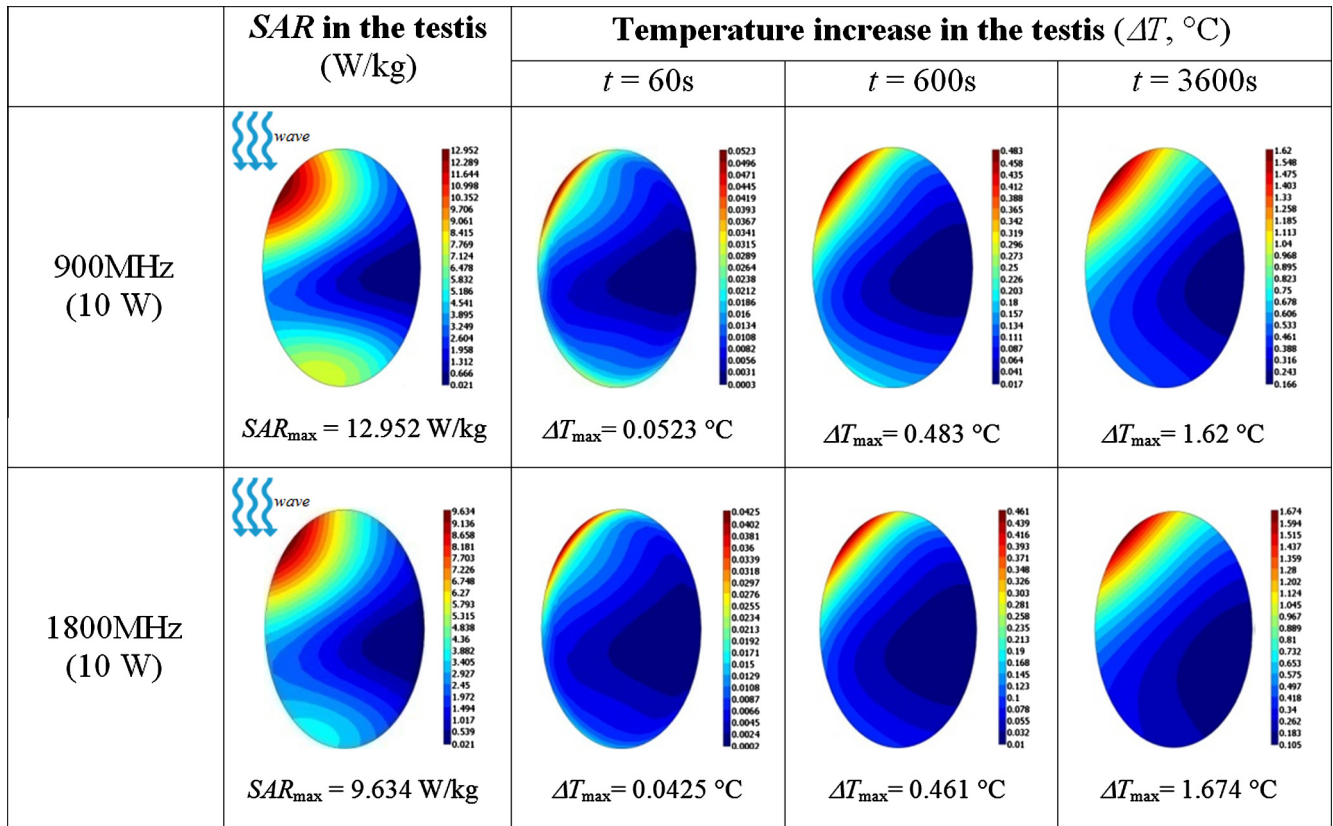


Fig. 11. Comparison between the distribution of SAR (W/kg) and temperature increase (°C) in testis during exposure to 900 and 1800 MHz EMF at various exposure times.

0.0523, 0.483, and 1.62 °C for the exposure times of 60 s, 600 s, and 3600 s, respectively. At the operating frequency of 1800 MHz, the maximum temperature increases are 0.0425, 0.461, and 1.674 °C for the exposure times of 60 s, 600 s, and 3600 s, respectively.

According to the higher SAR value of the testis at 900 MHz frequency, the absorbed energy of the 900 MHz case is also higher. A higher testis temperature increase at 900 MHz during the early period of exposure (60 s) is observed. Surprisingly, as time passes, the temperature increase in both frequencies shows almost no difference in the middle period (600 s). This is because not only the tissue's ability to absorb specific frequencies of EMF, but also the EM heating patterns and heat conduction in the surrounding tissues play an important role in heat transfer from the penis and scrotum to the testis. In the final period (3600 s), the stronger effect on the conduction from the surrounding tissue (induced by a larger temperature gradient) at 1800 MHz (Fig. 7b) has the result that the testis temperature increase at 1800 MHz is slightly higher than that at 900 MHz, even though the SAR value at 900 MHz is larger.

In this study, the maximum temperature increases in the testis exposed to the radiated power density of 10 W at the frequencies of 900 and 1800 MHz are 1.62 and 1.674 °C respectively. The temperature increases obtained may cause decreased sperm production [3]. It is found that the temperature increase distributions in the testis are not proportional to the local SAR values. Nevertheless, these are also related to parameters such as the surrounding tissue temperature, thermal conductivity, dielectric properties, blood perfusion rate, etc.

5. Conclusions

The numerical simulations of the electric field, SAR and temperature distributions in this study show several important features of

the energy absorption and temperature increase in the piecewise-homogeneous human model of the male reproductive organs and upper thigh during exposure to EMFs at 900 and 1800 MHz. This study indicated that when the model is exposed to EMFs at the frequencies of 900 and 1800 MHz, the highest SAR values are obtained in the scrotum. In the testis, the SAR value at 900 MHz is significantly higher than at 1800 MHz, while there are no significant differences in the temperature increases between the two operating frequencies.

The numerical simulations in this study show several important features of the energy absorption in the human tissue. The electric field distributions display a wavy behavior and show a strong dependence on the operating frequency and the dielectric properties of the tissue. The distribution patterns of the SAR vary corresponding to the electric field intensities. Besides the electric field intensity, the magnitude of the dielectric and thermal properties in each tissue type will directly affect the SAR distribution patterns. The SAR distribution at the frequency of 900 MHz shows a greater value of EM power absorption in deeper parts of the body and especially in the testis.

We refer to the SAR safety limit indicated in the Guidelines as 2 W/kg for general public exposure and 10 W/kg for occupational exposure according to ICNIRP. For the 2 W radiated power, the resulting SAR levels at both the 900 MHz and 1800 MHz frequencies do not exceed the occupational exposure limits of 10 W/kg specified in the ICNIRP. The calculated testis temperature increases are lower than the thresholds for the induction of infertility (1 °C) at both frequencies. However, in the case of 10 W radiated power, the SAR values are higher than the occupational exposure limits of 10 W/kg specified in the ICNIRP. The testis temperature increases also exceeded the threshold for the induction of infertility (1 °C) at both frequencies.

It is found that the temperature distributions in the testis are not directly proportional to the local SAR values due to the effect

of the interaction among parameters such as the thermal conductivity, dielectric properties, blood perfusion rate, etc. The results obtained may be of assistance in determining exposure limits for the power output of wireless transmitters, and their operating frequency for use with humans.

In future works, the effect of feed point position will be included in the analysis to represent the actual heat transfer process which occurs in a realistic situation and a more realistic 3D model will be developed for the simulations. This will allow a better understanding of the real situation of the interaction between EM fields and the human body.

Acknowledgments

The authors gratefully acknowledge the Thailand Research Fund (TRF) and Eastern Asia University (under the TRF contract No. TRG5780128).

References

- [1] R. Harrison, J. Weiner, Abdomino-testicular temperature gradients, *J. Physiol.* 18 (1948) 256–262.
- [2] P. Thonneau, L. Bujan, L. Multigner, R. Miesusset, Occupational heat exposure and male fertility: a review, *Hum. Reprod.* 13 (1998) 2122–2125.
- [3] K. Kumar, A.B. Raju, A review on male fertility, *Hygeia J. Drugs Med.* 3 (1) (2011) 20–28.
- [4] N.H.I. Hjollund, L. Storgaard, E. Ernst, J.P. Bonde, J. Olsen, The relationship between daily activities and scrotal temperature, *Reprod. Toxicol.* 16 (2002) 209–214.
- [5] E.J. Wright, G.P.H. Young, M. Goldstein, Reduction in testicular temperature after varicocele surgery in infertile men, *Urology* 2 (1997) 257–259.
- [6] Y. Sheynkin, R. Welliver, A. Winer, F. Hajimirzaee, H. Ahn, K. Lee, Protection from scrotal hyperthermia in laptop computer users, *Fertil. Steril.* 95 (2) (2011) 647–651.
- [7] D. Robinson, J. Rock, Intrascrotal hyperthermia induced by scrotal insulation: effect on spermatogenesis, *Obstet. Gynecol.* 2 (1967) 217–223.
- [8] K. Paulius, P. Napoles, P. Maguina, Thigh burn associated with laptop computer use, *J. Burn Care Res.* 29 (2008) 842–844.
- [9] C.G. Ostenson, Lap burn due to laptop computer, *Lancet* 360 (2002) 1704.
- [10] Y. Sheynkin, M. Jung, P. Yoo, D. Schulsinger, E. Komaroff, Increase in scrotal temperature in laptop computer users, *Hum. Reprod.* 20 (2005) 452–455.
- [11] C. Avendaño, A. Mata, C.A. Sanchez Sarmiento, G.F. Doncel, Use of laptop computers connected to internet through Wi-Fi decreases human sperm motility and increases sperm DNA fragmentation, *Andrology* 97 (1) (2012) 39–45.
- [12] International Commission on Non-Ionizing Radiation Protection: ICNIRP, Guidelines for limiting exposure to time-varying electric, magnetic and electromagnetic fields (up to 300 GHz), *Health Phys.* 74 (1998) 494–522.
- [13] H.H. Pennes, Analysis of tissue and arterial blood temperatures in the resting human forearm, *J. Appl. Phys.* 85 (1998) 5–34.
- [14] A.M. Seufi, S.S. Ibrahim, T.K. Elmaghraby, E.E. Hafez, Preventive effect of the flavonoid, quercetin, on hepatic cancer in rats via oxidant/antioxidant activity: molecular and histological evidences, *J. Exp. Clin. Cancer Res.* 28 (1) (2009) 80.
- [15] D. Yang, M.C. Converse, D.M. Mahvi, J.G. Webster, Measurement and analysis of tissue temperature during microwave liver ablation, *IEEE Trans. Biomed. Eng.* 54 (1) (2007) 150–155.
- [16] H. Kanai, H. Marushima, N. Kimura, T. Iwaki, M. Saito, H. Maehashi, K. Shimizu, M. Muto, T. Masaki, K. Ohkawa, K. Yokoyama, M. Nakayama, T. Harada, H. Hano, Y. Hataba, T. Fukuda, M. Nakamura, N. Totsuka, S. Ishikawa, Y. Unemura, Y. Ishii, K. Yanaga, T. Matsuura, Extracorporeal bioartificial liver using the radial-flow bioreactor in treatment of fatal experimental hepatic encephalopathy, *Artif. Organs* 31 (2) (2007) 148–151.
- [17] T. Wessapan, S. Srisawatdhisukul, P. Rattanadecho, Numerical analysis of specific absorption rate and heat transfer in the human body exposed to leakage electromagnetic field at 915 MHz and 2450 MHz, *ASME J. Heat Transfer* 133 (2011) 051101.
- [18] T. Wessapan, S. Srisawatdhisukul, P. Rattanadecho, The effects of dielectric shield on specific absorption rate and heat transfer in the human body exposed to leakage microwave energy, *Int. Commun. Heat Mass Transfer* 38 (2011) 255–262.
- [19] T. Wessapan, P. Rattanadecho, Numerical analysis of specific absorption rate and heat transfer in human head subjected to mobile phone radiation, *ASME J. Heat Transfer* 134 (2012) 121101.
- [20] T. Wessapan, S. Srisawatdhisukul, P. Rattanadecho, Specific absorption rate and temperature distributions in human head subjected to mobile phone radiation at different frequencies, *Int. J. Heat Mass Transfer* 55 (2012) 347–359.
- [21] P. Keangin, T. Wessapan, P. Rattanadecho, Analysis of heat transfer in deformed liver cancer modeling treated using a microwave coaxial antenna, *Appl. Therm. Eng.* 31 (16) (2011) 3243–3254.
- [22] P. Keangin, T. Wessapan, P. Rattanadecho, An analysis of heat transfer in liver tissue during microwave ablation using single and double slot antenna, *Int. Commun. Heat Mass Transfer* 38 (2011) 757–766.
- [23] P. Rattanadecho, P. Keangin, Numerical study of heat transfer and blood flow in two-layered porous liver tissue during microwave ablation process using single and double slot antenna, *Int. J. Heat Mass Transfer* 58 (2013) 457–470.
- [24] T. Wessapan, P. Rattanadecho, Specific absorption rate and temperature increase in human eye subjected to electromagnetic fields at 900 MHz, *ASME J. Heat Transfer* 134 (2012) 091101.
- [25] T. Wessapan, P. Rattanadecho, Specific absorption rate and temperature increase in the human eye due to electromagnetic fields exposure at different frequencies, *Int. J. Heat Mass Transfer* 64 (2013) 426–435.
- [26] T. Wessapan, P. Rattanadecho, Influence of ambient temperature on heat transfer in the human eye during exposure to electromagnetic fields at 900 MHz, *Int. J. Heat Mass Transfer* 70 (2014) 378–388.
- [27] T. Wessapan, P. Rattanadecho, Heat transfer analysis of the human eye during exposure to sauna therapy, *Numer. Heat Transfer, Part A* 68 (2015) 566–582.
- [28] P.J. Riu, K.R. Foster, Heating of tissue by near-field exposure to a dipole, *IEEE Trans. Biomed. Eng.* 46 (8) (1999) 911–917.
- [29] P.A. Hasgall, F. Di Gennaro, C. Baumgartner, E. Neufeld, M.C. Gosselin, D. Payne, A. Kligenböck, N. Kuster, IT'IS Database for thermal and electromagnetic parameters of biological tissues. Version 3.0, September 1st. 2015. <www.itis.ethz.ch/database>, DOI: <http://dx.doi.org/10.13099/VIP21000-03-0>.
- [30] S. Gabriel, R. Lau, C. Gabriel, The dielectric properties of biological tissues. II: Measurements in the frequency range 10 Hz to 20 GHz, *Phys. Med. Biol.* 41 (1996) 2251–2269.